Dimerization of aromatic ureido pyrimidinedione derivatives: observation of an unexpected tautomer in the solid state†

Lu Cui,[a] Suresh Gadde,[a] Atindra D. Shukla,[a] Hao Sun,[a] Joel T. Mague*[b] and Angel E. Kaifer*[a]

Received (in Cambridge, UK) 8th November 2007, Accepted 7th January 2008
First published as an Advance Article on the web 25th January 2008
DOI: 10.1039/b717285k

Ureido pyrimidinedione derivatives with phenyl, 1-naphthyl and 2-naphthyl substituents form stable dimers *via* quadruple hydrogen bonding, but the 1-naphthyl derivative presents an unexpected tautomer in the solid state.

The design and characterization of hydrogen bonding arrays is an important research topic within supramolecular chemistry.[1,2] A single hydrogen bond is usually too weak to provide a stable connection between two molecules and, thus, it is commonplace to design residues in which several hydrogen bonding donor or acceptor sites are arranged side by side to increase the enthalpic release upon association, as several, parallel hydrogen bonds form simultaneously.[3,4] In this regard the self-complementary ureidopyrimidine motif, developed by Meijer and co-workers[5] has attracted considerable attention. Its keto form presents a donor–donor–acceptor–acceptor (DDAA) array, which gives rise to highly stable dimers. A complication usually observed with this hydrogen bonding motif is the presence of its tautomeric enol form (DADA), which, as expected, gives rise to weaker dimers. Corbin and Zimmerman have reported structural variations to improve on this problem.[6] In 2005, Sanjayan and co-workers proposed a ureido pyrimidinedione motif (DDAA),[7] capable of forming stable dimers without complications derived from the existence of tautomeric forms. We recently prepared a ferrocenyl ureido pyrimidinedione derivative that has interesting electrochemical properties.[8] Intrigued by these results, we started a systematic investigation of aromatic ureido pyrimidinedione derivatives. Here, we report on the properties of pyrimidinedione compounds with phenyl, 1-naphthyl and 2-naphthyl groups directly attached *via* a ureido linkage (Scheme 1). All three compounds form stable dimers, although one of them exhibits an unexpected tautomeric form in the solid state.

The preparation of the aromatic pyrimidinedione derivatives (**2–4**) is shown in Scheme 1. Each of the commercially available isocyanates were reacted with amine **1**, which was prepared as reported before.[7] The self-complementary aromatic products, containing a DDAA hydrogen bonding array, were obtained in modest yields, as a result of the low reactivity of heterocyclic amines, such as **1**, with isocyanates.[4] Full synthetic details and characterization data are given in the ESI.† The ^{1}H NMR spectra of all these compounds is consistent with the presence of dimeric assemblies in $CDCl_3$ solution, as evidenced by the three downfield-shifted NH proton resonances, reflecting their engagement in hydrogen bonds. Fig. 1 shows the spectrum of the phenyl derivative (compound **2**) in which the hydrogen-bonded NH protons appear at 12.7, 11.3 and 10.5 ppm. Similar spectra were obtained with **3** and **4** in $CDCl_3$ as well as for **2–4** in CD_2Cl_2 solution.

In order to assess the stability of these dimers we monitored the chemical shifts of the three NH protons as a function of temperature with samples of $\mathbf{2}_2$ in $CDCl_3$ solution. We found that the chemical shift of the lowest field NH proton is not very sensitive to temperature in the range 25–50 °C [δ(ppm) = 12.73 − 0.006T (°C)]. In clear contrast to this, the other two NH protons exhibit greater temperature sensitivity: δ(ppm) = 11.74 − 0.025T(°C) and δ(ppm) = 10.88 − 0.023T (°C). The displacement of all the NH resonances to higher field with increasing temperature is consistent with a decreasing proportion of dimer in the equilibrium mixture. However, the small temperature sensitivity of the lowest field NH proton reveals that this peak corresponds to the intramolecular hydrogen bond, while the remaining two NH peaks correspond to the intermolecular hydrogen bonds primarily responsible for the formation of the dimer. Similar data were obtained in dilution experiments with **2–4** in $CDCl_3$ solution. In this case, lowering

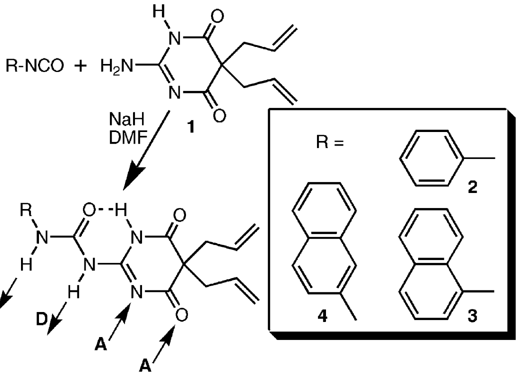

Scheme 1 Synthesis of the self-complementary compounds surveyed in this work. The DDAA hydrogen bonding array on the product is indicated by arrows.

---

[a] Center for Supramolecular Science and Department of Chemistry, University of Miami, Coral Gables, FL 33124-0431, USA. E-mail: akaifer@miami.edu; Fax: 1-305-284-4571; Tel: 1-305-284-3468
[b] Department of Chemistry, Tulane University, New Orleans, LA 70118, USA. E-mail: joelt@tulane.edu

† Electronic supplementary information (ESI) available: Synthetic details and spectroscopic characterization data for compounds **2**, **3** and **4**. X-Ray experimental details. Plots of chemical shift for the NH protons of **3** and **4** *vs.* temperature and concentration. See DOI: 10.1039/b717285k

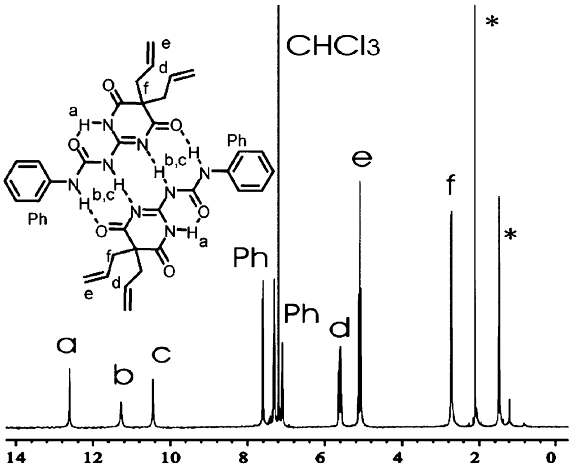

Fig. 1 ^{1}H NMR (400 MHz, RT) spectrum of compound **2** (12 mM) in $CDCl_3$ solution. The symbol '*' denotes residual solvent peaks.

the analytical concentration of the DDAA compound should increase the [monomer]/[dimer] ratio and shift the NH proton resonances to higher field. We did observe upfield shifts for all the NH proton signals on dilution, but the magnitude of the shift was very small in the case of the lowest field NH proton (confirming its engagement in an intramolecular hydrogen bond) and more pronounced in the case of the other two NH protons. Since the chemical shift (δ_{obs}) of the latter protons can be expressed as

$$\delta_{obs} = \delta_m x_m + \delta_d x_d \quad (1)$$

where the subscripts 'm' and 'd' refer to monomer and dimer, respectively, we fitted the experimental data using regression analysis (see ESI† for illustrative examples) to obtain the equilibrium constants for the dimerization process (K_{dim}). The resulting values are given in Table 1. Vapor pressure osmometry (VPO) measurements were also utilized to determine the effective molecular weights of the solutes in $CHCl_3$ solution. The results (Table 1) also indicate that the predominant solution species is the dimer in all cases.

Compounds **2–4** formed single crystals of sufficient quality for X-ray diffraction studies.‡ All three compounds were found to crystallize as hydrogen-bound dimers, and representative dimer structures are shown in Fig. 2. Interestingly compound **2** and **4** self-recognize in the solid state, forming dimers through DDAA hydrogen bonding arrays, but compound **3** dimerizes as a tautomeric DADA array. This is a surprising result, not only because these pyrimidinedione derivatives were designed to avoid tautomerization, but also because DDAA dimers are known to be more stable than DADA dimers, due to repulsive secondary interactions[9,10] between the four parallel hydrogen bonds in the latter case. Despite final *wR*2 being somewhat larger in **3** (0.144) than in **2** (0.097) and **4** (0.117), hydrogen atoms attached to nitrogen atoms were clearly visible in difference maps for all three structures and their positional and isotropic displacements were satisfactorily refined. Furthermore, both endocyclic C–N bond distances in **3** were identical within experimental error [average: 1.365(2) Å] while the exocyclic C–N distance was much shorter [1.304(2) Å]. In **4**, one of the endocyclic C–N distances was identical to the exocyclic C–N distance [average: 1.356(2) Å], while the other endocyclic C–N distance was shorter [1.319(2) Å]. A similar situation was seen in **2**. All these data strongly support the hydrogen atom positions shown in Fig. 2. Additionally, it can be noted that, for compounds **2** and **4**, the aromatic residues align themselves almost perfectly with the plane formed by the four hydrogen bonds. Again compound **3** is the exception, as the naphthyl groups are clearly twisted away from the hydrogen bonding plane (see ESI†). The two naphthyl derivatives (**3** and **4**) crystallize in the same space group but the unit cell of the 1-naphthyl compound (**3**) is smaller by *ca.* 200 Å^3. Therefore, in the solid state, the degree of packing and the density are higher in **3** as compared to **4**. Some representative atomic distances in these crystals are listed in Table 2. The intermolecular H–O hydrogen bonding distance is larger in the $\mathbf{3}_2$ dimer than in the other two dimers, in agreement with the weaker binding energy expected for DADA dimers compared to DDAA dimers. However, these differences are attenuated in the intermolecular N–H distances, whereas the intramolecular O–H hydrogen bond, which rigidifies these structures and facilitates the formation of the four intermolecular hydrogen bonds, is in fact shorter in $\mathbf{3}_2$ than in the other two dimers.

Table 1 Dimerization data for compounds **2–4** in chloroform solution at 25 °C

Compound	K_{dim}/M^{-1}	MW^a (exptl.)	MW^b (calc.)
2	2.0×10^4	652	656
3	7.4×10^3	762	752
4	2.1×10^5	674	752

[a] Measured in VPO experiments. Calibration curves were obtained using biphenyl as a MW standard. [b] Calculated for the dimer.

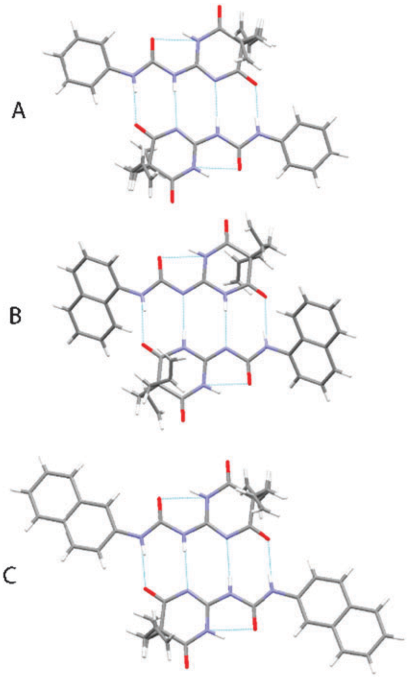

Fig. 2 X-Ray crystal structures of (A) compound **2**, (B) compound **3**, and (C) compound **4**.

Table 2 Representative distances (Å) and angles in the crystal structures of compounds **2–4**

Compound	d_{H-O}[a]	d_{H-N}[b]	d_{H-O}[c]	Angle[d]/°
2	1.889(17)	2.153(16)	1.842(17)	178.4(1)
3	2.05(2)	2.16(3)	1.74(3)	143.2(1)
4	1.881(18)	2.147(18)	1.76(2)	179.8(1)

[a] H–O intermolecular hydrogen bond distance. [b] H–N intermolecular hydrogen bond distance. [c] H–O intramolecular hydrogen bond distance. [d] Dihedral angle between the aromatic residue and the H-bonding plane.

We also performed DFT calculations (using the B3LYP method with a 3-21G* basis set[11]) on the monomeric and dimeric forms of compounds **3** and **4** in an attempt to rationalize the observation of the DADA tautomer in the crystal structure of $\mathbf{3}_2$. These calculations were done for all compounds in their DDAA and DADA tautomers. Starting geometries for the computational work were taken from the X-ray crystal structural data. A summary of the results is collected in Table 3.

A comparison between the hydrogen bonding distances determined experimentally from the X-ray crystal data (Table 2) and those obtained computationally (Table 3) reveals that the latter are uniformly shorter. This finding is easily rationalized by considering that the computational work does not take into account the presence of solvent molecules and, thus, electrostatic attractive interactions, such as hydrogen bonding, are expected to be overemphasized. However, the data set in Table 3 is self-consistent and we can draw useful conclusions from its examination. For instance, in all cases, the H–O intermolecular hydrogen bond distances are shorter in dimers formed between DDAA tautomers than in those formed by DADA tautomers. The same trend, although the bond length differences are less pronounced, holds for the H–N intermolecular hydrogen bond distances. These findings are consistent with the already mentioned greater stability of dimers formed by self-recognition of DDAA hydrogen bonding arrays *vs.* those formed by DADA arrays. In contrast to this, our DFT computations suggest that the intramolecular hydrogen bond, which rigidifies the monomers favoring the formation of four intermolecular hydrogen bonds, is in fact slightly shorter in the case of DADA tautomeric arrays, in agreement with the experimental X-ray data.

Table 3 Representative distances (Å), angles and energies of formation (kcal mol^{-1}) calculated for dimers formed by compounds **2–4** using DFT methods

Comp. (tautomer)	d_{H-O}[a]	d_{H-N}[b]	d_{H-O}[c]	Angle[d]
2 (DDAA)	1.644	1.826	1.658	179
2 (DADA)	1.712	1.870	1.642	179
3 (DDAA)	1.662	1.813	1.637	154
3 (DADA)	1.720	1.856	1.633	153
4 (DDAA)	1.642	1.831	1.659	180
4 (DADA)	1.707	1.880	1.641	180

Comp. (tautomer)	$\Delta_f E$ (monomer)	$\Delta_f E$ (dimer)	$\Delta_{dim}E$[e]
2 (DDAA)	−688 551.6	−1 377 173.8	
2 (DADA)	−688 564.1	−1 377 174.0	−45.8
3 (DDAA)	−784 430.4	−1 568 925.8	
3 (DADA)	−784 443.1	−1 568 925.5	−39.6
4 (DDAA)	−784 431.8	−1 568 935.9	
4 (DADA)	−784 444.7	−1 568 935.1	−46.5

[a] H–O intermolecular hydrogen bond distance. [b] H–N intermolecular hydrogen bond distance. [c] H–O intramolecular hydrogen bond distance. [d] Dihedral angle between the aromatic residue and the hydrogen bonding plane. [e] Calculated as $\Delta_{dim}E = \Delta_f E(\text{dimer}) - 2\Delta_f E(\text{monomer})$ using the most stable dimer/monomer forms for each compound.

Table 3 also lists the formation energies obtained from the optimization of these structures. For each of the monomers, more energy is released in the formation of the DADA tautomer than in the formation of the corresponding DDAA form. This is again expected, due to the minimization of electrostatic repulsions in the DADA forms. However, upon dimerization, DDAA dimers are generally found to be slightly more stable than their DADA counterparts. However, the calculated energy of dimerization is clearly smaller in the case of compound **3** (1-naphthyl derivative) than for the other two compounds. Since in the crystal structure of dimer $\mathbf{3}_2$ the naphthyl groups are twisted out of the hydrogen bonding plane we also run a number of computations exploring the effect of variable dihedral angles. The results showed minimal variations compared to the data given in Table 2. At this point the observed DADA tautomer in the crystal structure of the $\mathbf{3}_2$ dimer can only be justified partially by the results of these DFT calculations, which lead us to suggest that crystal packing factors should play an important role in this particular crystal structure.

In conclusion, we have shown that aromatic ureido pyrimidinedione derivatives **2–4** self-recognize, forming stable dimers, assisted by the formation of two intramolecular hydrogen bonds, which increase the structural rigidity of each monomer and facilitate the formation of four parallel intermolecular hydrogen bonds. Surprisingly, one of the dimers ($\mathbf{3}_2$) crystallizes in the DADA tautomeric form, while the other two crystallize in their DDAA forms. The $|\Delta_{dim}E|$ value for $\mathbf{3}_2$ was found to be significantly smaller than those for $\mathbf{2}_2$ and $\mathbf{4}_2$. This fact combined with the higher degree of crystal packing found in the solid-state structure of $\mathbf{3}_2$ are probably the most important factors behind the observation of the unexpected tautomeric form.

Notes and references

‡ CCDC 670607–670609. For crystallographic data in CIF or other electronic format see DOI: 10.1039/b717285k

1 L. J. Prins, D. N. Reinhoudt and P. Timmerman, *Angew. Chem., Int. Ed.*, 2001, **40**, 2382.
2 J. L. Sessler and J. Jayawickramarajah, *Chem. Commun.*, 2005, 1939.
3 R. P. Sijbesma and E. W. Meijer, *Chem. Commun.*, 2003, 5.
4 T. Park, E. M. Todd, S. Nakashima and S. C. Zimmerman, *J. Am. Chem. Soc.*, 2005, **127**, 18133.
5 F. H. Beijer, R. P. Sijbesma, H. Kooijman, A. L. Spek and E. W. Meijer, *J. Am. Chem. Soc.*, 1998, **120**, 6761.
6 P. S. Corbin and S. C. Zimmerman, *J. Am. Chem. Soc.*, 1998, **120**, 9710.
7 P. K. Baruah, R. Gonnade, U. D. Phalgune and G. J. Sanjayan, *J. Org. Chem.*, 2005, **70**, 6461.
8 H. Sun, J. Steeb and A. E. Kaifer, *J. Am. Chem. Soc.*, 2006, **128**, 2820.
9 W. L. Jorgenson and J. Pranata, *J. Am. Chem. Soc.*, 1990, **112**, 2008.
10 J. Pranata, S. G. Wierschke and W. L. Jorgenson, *J. Am. Chem. Soc.*, 1991, **113**, 2810.
11 M. E. Zandler and F. D'Souza, *C. R. Chim.*, 2006, **9**, 960.